Final Technical Report

Federal Agency and Organization Element:
U.S. Department of Energy National Energy Technology Laboratory

Federal Grant or Identification Number: **DE-EE0007757**

Project Title: **High Speed Hybrid Reluctance Motor Utilizing Anisotropic Materials**

Principal Investigator: **Edwin Chang,** (248) 310-7056
edwin.chang@gm.com
Technical Core Member: **Jihyun Kim,** (248) 563-1194
jihyun.kim@gm.com
Business Point of Contact: **Sean Campbell,** (248) 296-4128
Sean.c.campbell@gm.com

Submission Date: **March 31, 2021**
DUNS Number: 076336064

Recipient Organization:
General Motors LLC
850 N. Glenwood Ave
Pontiac, MI 48340-2920

Partner Organizations: Oakridge National Laboratory

Submitting Official: Sean C. Campbell – Government Contracts Manager

Acknowledgment: This material is based upon work supported by the Department of Energy, Office of Energy Efficiency and Renewable Energy (EERE), under Award Number DE-EE0007757.

Acronyms, Abbreviations, Symbols, and Units

BoM – Bill of Materials

BoP – Bill of Process

FEA – Finite Element Analysis

GOES – Grain Oriented Electrical Steel

HRE – Heavy Rare Earth

NOES – Non-oriented Electrical Steel

PM – Permanent Magnet

RE – Rare Earth

SyRM – Synchronous Reluctance Motor

EXECUTIVE SUMMARY

With high cost and volatility driving continued efforts to decrease reliance on the critical heavy rare earth materials used in traction drive applications, General Motors developed three variants of heavy rare earth-free (HRE-free) electric motors. The variants focused on taking advantage of advanced magnet technologies and new rotor topologies to improve mechanical strength and achieve power targets. The three variants were a HRE-free permanent magnet reluctance motor, a synchronous reluctance motor utilizing small HRE-free permanent magnets, and an induction motor with inserted copper bars and cast aluminum end-rings. Motors were designed with the intent of primary or secondary traction applications, depending on the topology.

Variant 1 achieved performance comparable to HRE-containing permanent magnet motors through optimized topology and validation of HRE-free magnets, focusing on achieving energy products and demagnetization resistance comparable to those of HRE-containing magnets. Demagnetization testing demonstrated the motor robustness to currents and temperatures exceeding expected vehicle conditions, a key challenge to the use of HRE-free magnets. The Variant 1 motor also showed the best capability of meeting the US Drive technology 2020 targets, due to the high power-density of the permanent magnet motor and the potential cost reductions enabled by the removal of heavy rare earth materials.

Variant 2 exhibited high efficiency in high speed regions due to the low high-speed losses, an important consideration for secondary traction applications, and significantly thrifted on magnet mass to reduce cost.

Variant 3 contained copper bars within the induction rotor to reduce losses compared to cast aluminum, while using cast aluminum end-rings to reduce the cost and mass of the rotor. Optimization of the Cu-Al interface were focused on, as the interface is prone to forming brittle intermetallic compounds during the casting process.

Prototypes of each motor variant were built and tested for performance, mechanical strength, and demagnetization resistance (Variants 1 and 2 only), with torque and power resulting close to the

predicted values.

GOALS and OBJECTIVES

Three motor design types were studied to determine the feasibility of each approach. These three motor variants were selected based on their expected ability to meet the technical targets. These design approaches took advantage of material advancements which allow these motors to meet the performance requirements without heavy rare earth elements or rare earth elements altogether.

The project concentrated on four major tasks. Budget Period 1 covered Tasks 1 and 2, Budget Period 2 covered Task 3, and Budget Period 3 covered Task 4.

Task 1: Material Evaluation and Selection

Task 2: Electromagnetic and Mechanical Machine Design

Task 3: Electric Motor Prototype Manufacturing

Task 4: Verification Testing and Performance Evaluation

Task 1: Material Evaluation and Selection

- Development of the requirements for Grain Oriented Electrical Steel (GOES)
- Survey of available grades of GOES
- Industry survey of GOES available grades and Selection for Electromagnetic Design Studies
- Execution of FEA-based design studies for Synchronous Reluctance Motor using GOES, and Hybrid Synchronous Reluctance Motor using Anisotropic HRE-free magnets and GOES
- Development of, working with suppliers, HRE-free anisotropic magnet material
- Evaluation of the developed anisotropic HRE-free magnets and Non-Oriented Electrical Steel (NOES) for use in the motor laminations.

Task 2: Electromagnetic and Mechanical Design of 3 Machines

- Detailed structural, thermal, and electromagnetic analysis of the machine concepts to ensure that the motors meet both the performance and reliability objectives required for use in General Motor's electrified vehicle portfolio
- Generation of an Indentured Bill of Materials (BoM)

Task 3: Electric Motor Prototype Manufacturing

- Prototype motors were built to ensure that they met all GM Production Bill of Process (BoP) requirements
- Production Manufacturing Equipment identified and associated costs were documented
- Comprehensive test plan for machine verification were defined and durability test plans for

demonstration were developed

Task 4: Verification Testing and Performance Evaluation

- All three motor designs were calibrated for peak torque and efficiency
- Machines were tested for performance and efficiency verification
- Torque and power vs. speed curves were generated
- Complete efficiency maps for both motoring and generating were generated for operations at different voltage levels
- Measured performance maps were compared to the predicted results for data correlation purposes
- Rotor durability testing executed on two variants (Synchronous Reluctance motor with HRE-free Magnet Assist and High Performance Hybrid Induction Motor using Inserted Copper Bars and Aluminum Die Cast End-rings) and included rotor speed cycling at various RPM to induce fatigue failures in the rotor laminations
- The HRE-free PM motor variant was excluded from rotor durability testing due to its similarity to other production designs that had previously demonstrated superior reliability

Oak Ridge National Laboratory (ORNL) a co-recipient of this project, was responsible for aspects of materials testing. ORNL's objectives were to characterize material properties of electrical steels and cast Al to Cu bar interfaces.

ACCOMPLISHMENTS

Materials Testing and Evaluation

GOES Industry Survey: Preliminary Selection and Initial Motor Design Studies

An industry survey was conducted with, but not limited to, electrical steel suppliers with whom GM has extensive experience of working with on production and development projects for non-grain-oriented steels. The best available steels were compared across suppliers, based on their provided data. In addition, calculations were carried out based on available academic knowledge to understand theoretical limits of saturation flux density and performance of grain-oriented steels. Targets were set for material improvement based on these results.

Detailed design studies were carried out using grain-oriented steel in the rotor as well as in the stator. The goal of these design studies was to increase motor torque density and subsequent increase in efficiency. Several rotor geometries were fully optimized using GOES in different orientations. Some of these studied also included GOES in the stator. Motor manufacturability and cost were specifically studied.

These extensive design studies with the introduction of GOES in the rotor only resulted in a modest (<3%) increase in motor torque. In addition, designs optimized for best electromagnetic performance were largely not manufacturable. Improvement in torque was best realized through the substitution of grain-oriented steel in the stator. However, this was not only difficult to manufacture but also deemed to be cost-

prohibitive.

Due to the limited success with the increase of motor performance with GOES it was decided to discontinue any additional design efforts using GOES. The project goal was re-scoped with more promising technologies.

HRE-Free Magnet Testing

HRE thrifting and eventual total elimination is a major goal toward which GM is working in conjunction with several major magnet suppliers. Significant advancements have been made in recent years with HRE-free magnet development. Several anisotropic magnet processing technologies show promise in increasing magnet coercivity without HRE material, which is critical for surviving demagnetization at elevated temperature. This has enabled the investigation of HRE-free magnets for traction motor applications. A few properties of promising HRE-free magnets are compared in Figure 1 with a more conventional baseline magnet with HRE additives. Magnet coercivity of some of the HRE-free magnets is comparable or even higher than those of other more conventional HRE magnets. The increase in coercivity of HRE-free magnet is often achieved at the expense of residual flux density as shown in Figure 1. This is one area the magnet manufacturers are working to overcome. Lower remanence requires the magnet to compensate for lower energy, thus increasing magnet cost. Nevertheless, the HRE-free magnets are crucial to overcome the supply and price volatility of HRE magnet materials which is a major concern for the automotive industry.

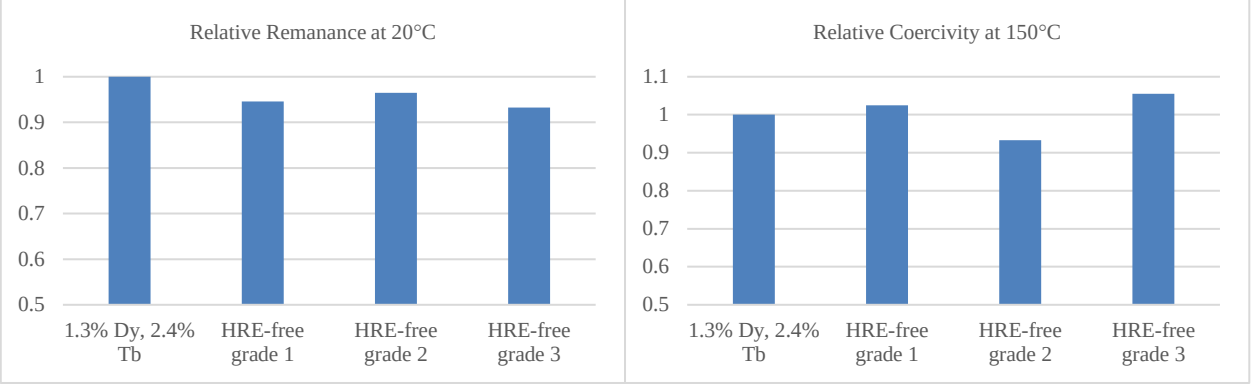

Figure 1: Magnetic Properties (GM testing)

Non-Oriented Electrical Steel (NOES) Selection

General Motors has been working with major steel suppliers towards the development of non-oriented electrical steel (NOES) with high permeability, low iron loss, and high mechanical strength. GM has set a target for electrical steel for EV and plug-in hybrid applications based on the motor operation's standard drive cycles. Non-oriented electrical steels used in the Synchronous Reluctance Motor (SRM) and HRE-free interior PM (IPM) Motor were selected based on these magnetic and mechanical properties. Table 1 compares the magnetic and material properties of a few 0.27 mm thick steels from major steel suppliers developed towards GM set targets. GM conducted standard Epstein and tensile tests internally to estimate magnetic and mechanical properties respectively as listed in Table 1. Final sourcing for prototype builds depended on the optimized electric motor performance of these steels for standard vehicle drive cycles and on material availability.

Induction motors require high permeability electrical steel to minimize excitation energy while building the rotor magnetic field. GM has been working with electrical steel suppliers to develop steels specifically for induction motors. NOES used in the induction motor was selected for high permeability and reasonably low iron losses and good mechanical strength. A survey of 0.3mm thick NOES with the best permeability properties across leading steel mills was conducted and results were compared based on supplier provided data. Two high performing steels were identified based on these criteria and were selected based on material availability during sourcing for prototype builds.

Supplier	Supplier A	Supplier B	Supplier C	Supplier D
Grade	Grade A	Grade B	Grade C	Grade D
Thickness	0.27 mm			
Iron loss, W10/400 (W/kg)	11.7	12.2	11.4	12.0
Flux density, B50 (T)	1.67	1.67	1.68	1.67
Yield strength, YS (MPa)	417	420	431	413

Table 1: Steel Evaluation Data of 0.27mm Steel

Copper-Aluminum Bar Interface Testing

The predominant method of induction rotor construction for traction motor applications is die-cast with aluminum. Copper rotors are built, to improve efficiency and rotor thermal performance, by fabricating copper bars and welding copper end-rings after bar insertion. GM is pursuing a new rotor manufacturing method where aluminum end-rings are die-cast to make electrical connections with the inserted copper bars resulting in a hybrid aluminum-copper rotor. To confirm the robustness of the Cu-Al interface, thermal shock and fatigue testing was performed. The thermal shock testing demonstrated no difference between the coated copper bars and bare copper bars. However, the coated copper bars performed significantly better in fatigue cycling, demonstrating improvements in robustness to mechanical stress. The objective is to replicate these characteristics for all bars in a die cast aluminum ring rotor. Table 2 shows the Cu-Al bar test results.

	Stress (MPa)	Average Cycles to Failure	Failure Location
Coated Cu-Al bar	161	360000	Copper Broke at aluminum

Coated Cu-Al bar	175	235000	Copper Broke at aluminum
Coated Cu-Al bar	189	87000	Copper Broke at aluminum
Bare Cu-Al bar	175	16000	Copper pulled out at aluminum

Table 2: Cu-Al Bar Test Results

Electromagnetic and Mechanical Motor Design of 3 Machines

The electromagnetic design has shown that the motor variants are capable of exceeding the DoE 2020 goals for performance. Table 3 shows a summary of the motor performances of the three machine variants. DoE target and overview of GM designed motors is also listed in Table 3.

Criteria	HRE-free PM Motor	Synchronous Relucance Motor with HRE-free PM Assist	Hybrid Induction Motor with Insert Cu Bars and Cast Al End-rings
Stator Outer Diameter (mm)	208	190	190
Stator Core Length (mm)	200	100	100
Power (kW)	150	86	86
Torque (N-m)	360	255	328
Max RPM	12000	16650	14000

Table 3: Motor Design Targets

The Variant 1 motor was a two-layer V permanent magnet design using HRE-free neodymium-iron-boron (NdFeB) magnets. Figure 2 shows the lamination 2D design and the power-speed and torque-speed curves of the motor. Despite lower magnet coercivity due to the HRE-free composition compared to HRE-containing magnets, the resistance to demagnetization was shown to be acceptable based on FEA results.

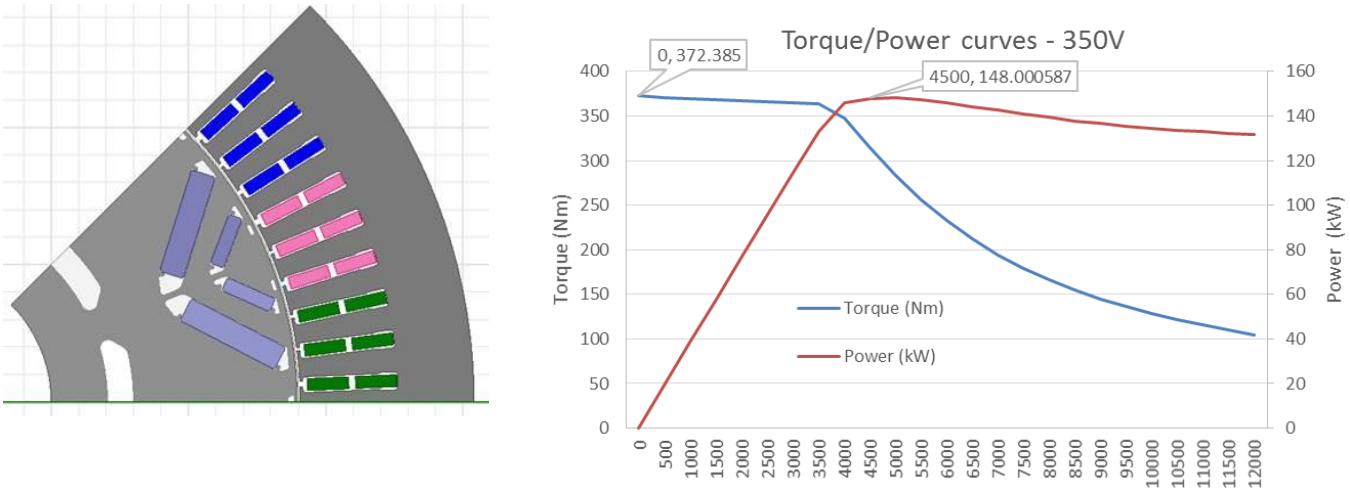

Figure 2: Variant 1 2D lamination design, left. Torque-speed and power-speed curves, right.

Variant 2 was achieved using a four-barrier design and stress relief features in the rotor webs to enable mechanical strength at higher speeds. Small HRE-free magnets provide magnetic saturation of the rotor webs. Optimization of the topology, including stress-relief features, was required in order to balance the requirements of low magnet mass, higher torque, and mechanical strength. The 2D lamination design, torque-speed curve, and power-speed curve are shown in Figure 3.

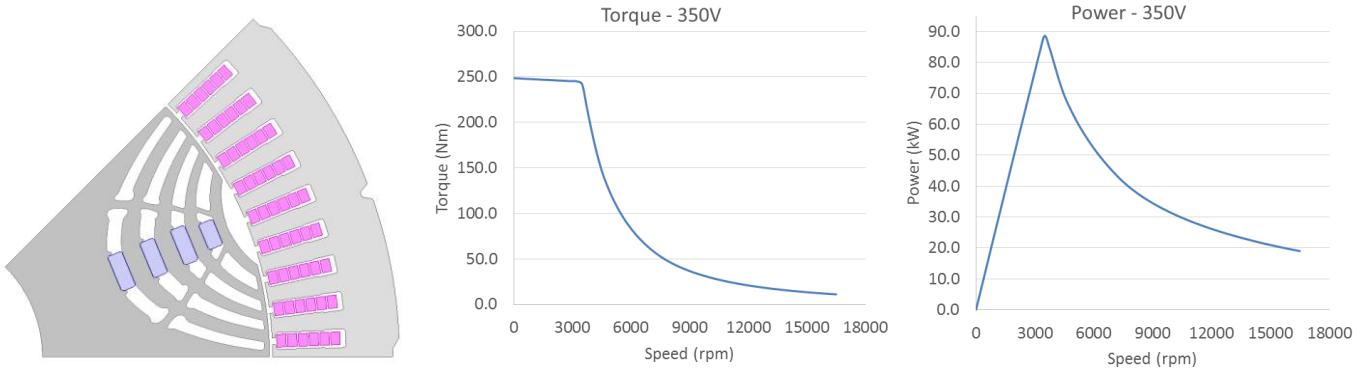

Figure 3: Variant 3 2D lamination design, left. Torque-speed and power-speed curves, right.

Variant 3 implemented inserted copper bars and aluminum end-rings. The aluminum end-rings enable lower cost while the copper bars enable lower losses in the slots, resulting in higher continuous torque. The 2D structure is shown in Figure 4, along with the continuous torque comparison.

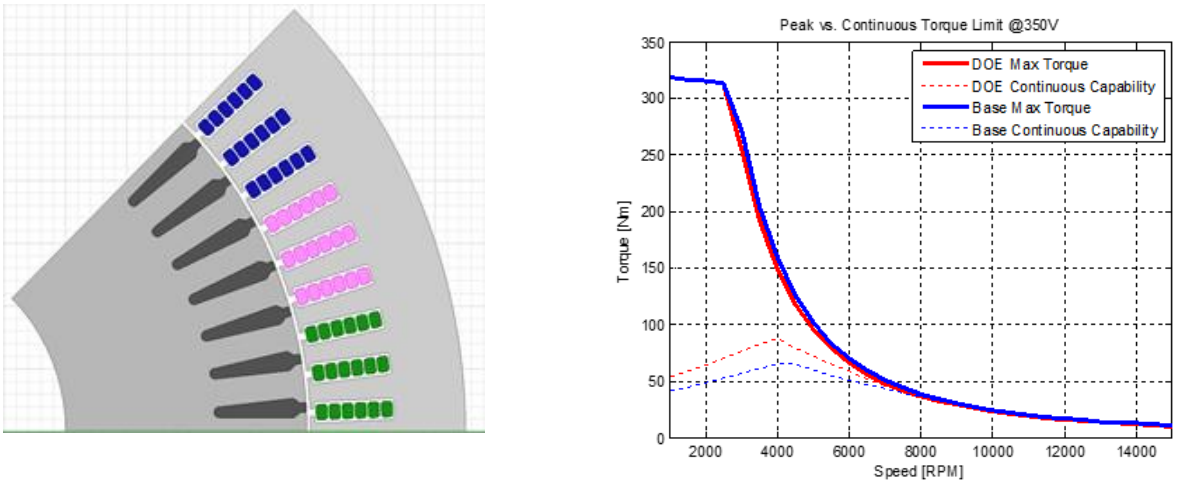

Figure 4: Variant 3 2D lamination design, left. Torque-speed and power-speed curves, right with comparison to baseline design continuous operation.

Motor Manufacturing

General Motors identified and worked with key suppliers to source and produce the subcomponents required. Stators for the HRE-free PM motor and Cu-Al hybrid induction motor were manufactured by GM Global Propulsion Systems in Pontiac and are shown in Figure 5. The stamping of the HRE-free PM rotor cores and SyRM with small HRE-free PM assist rotors were completed on progressive dies. The method of stamping and interlocking were chosen as this was determined to be most comparable in mechanical performance to production baseline designs. Aluminum castings of the hybrid Cu-Al induction motors were completed on horizontal die-casting equipment. The mold was designed using casting flow simulations. Final assemblies of the rotors are shown in Figure 6.

Figure 5: Variant 1, 2, and 3 stators shown from left to right

Figure 6: Variant 1, 2, and 3 rotors shown from left to right

Although concerns were present for the magnetization of the HRE-free PM machine due to the position and microstructure of the HRE-free magnets, finite element analysis results showed that the rotor would be able to be magnetized using standard magnetization equipment without necessary upgrades.

Due to manufacturing restrictions related to the slot fill of the stators, the stator for Variant 2 and Variant 3 had to be modified from the original design by decreasing the slot tooth size. This led to a small reduction in torque at low speeds, but resulting in no change in the peak power or the motor ability to meet the DoE power targets. The results of this design change are shown below in Figure 7.

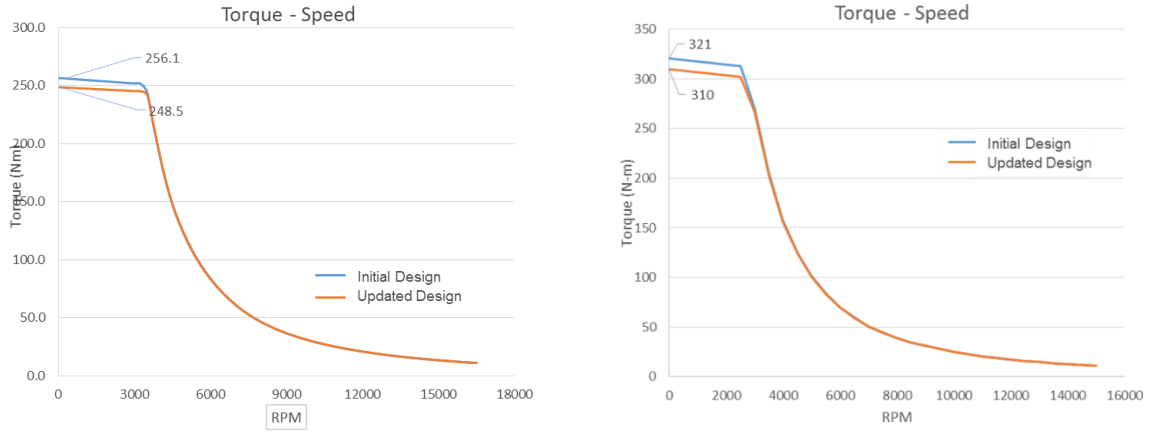

Figure 7: Variant 2, left, and Variant 3, right, power loss due to slot tooth width decrease

Significant development was performed to improve the casting results of Variant 3. Simulations were performed as shown in Figure 8 to aid in tooling design. Initial casting results showed significant variation in bar-to-bar quality as measured by tensile testing to evaluate the Al-Cu interface quality. Microscopic examination of the Al-Cu interfaces showed significant variation, gaps in the interface due to shrinkage, and overall poor interface quality. As the rotor quality is dependent on defect reduction, a design of experiment was created varying bar length, casting parameters, and flux, leading to a 33% improvement in bar retentions over the baseline design, as shown in Figure 10.

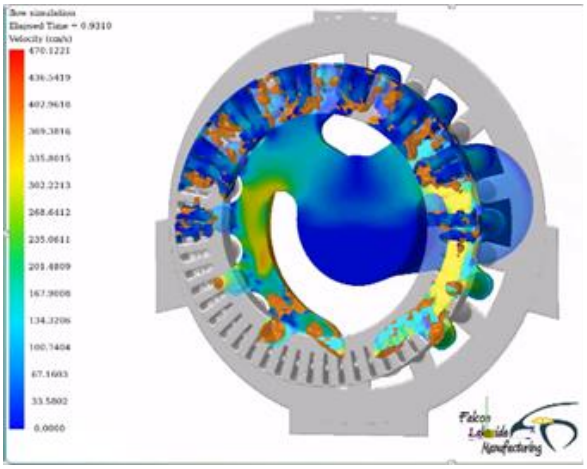

Figure 8: Rotor casting simulations for improved Al-Cu interface strength

Figure 9: Rotor test coupons and test setup from casting development

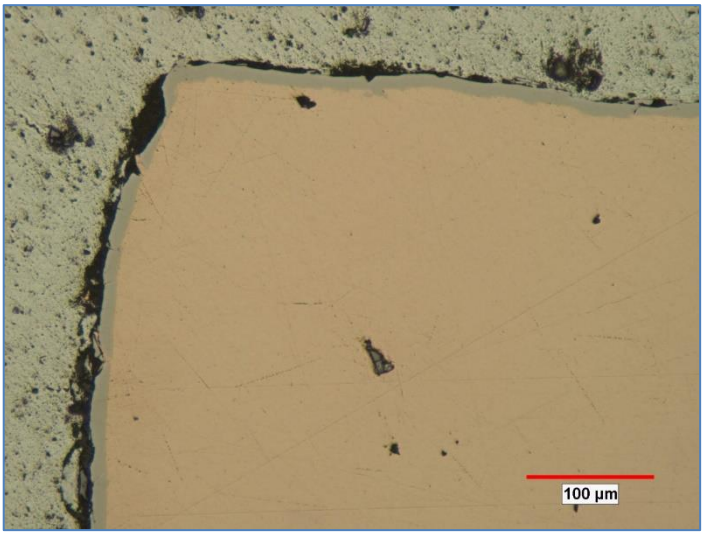

Figure 10: Microscopic view of copper bar to aluminum interface, showing gaps at the interface

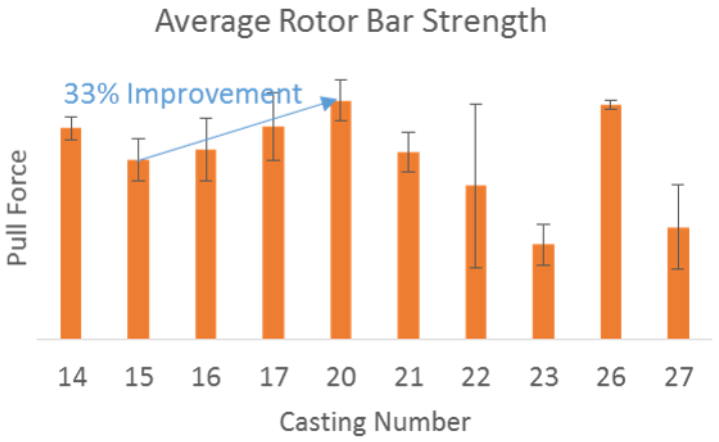

Figure 11: Average rotor bar improvement from baseline (Casting #15) based on pull force. Casting numbers represent different parameters in the design of experiment

Cost analysis

GM completed initial cost analysis showing that while the DoE cost target of $4.7/kW was met for the Variant 1, significant challenges were still found to meeting the DoE 2020 cost target with Variant 2 and Variant 3. Variant 1 had reduced cost due to the removal of the HRE cost of the magnets, but the Variant 2 and Variant 3 motors were challenged by the lower power densities of each motor. The cost estimate breakdown is shown below in Figure 12. Manufacturing analysis, including floor plans, tooling estimates, and required headcount were completed.

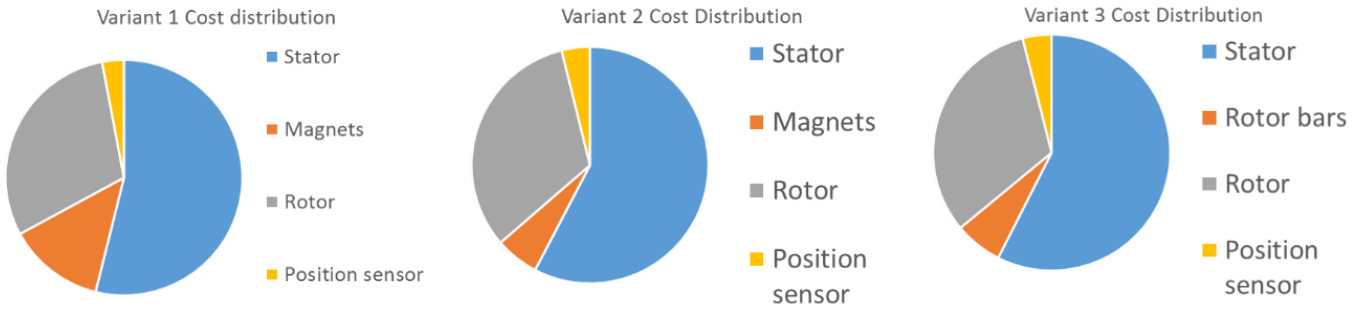

Figure 12: Cost breakdown of Variants 1, 2, and 3. Variant 1 only was estimated to be below the DoE cost target of $4.7/kW.

Motor Testing

Demagnetization testing of rotors was performed to better set the requirements for demagnetization. The testing was completed for rotors containing three different levels of coercivity, each showing three steps of demagnetization of the rotor. The demagnetization was then correlated with the test results, which will lead to better demagnetization predictions and more accurate motor protection.

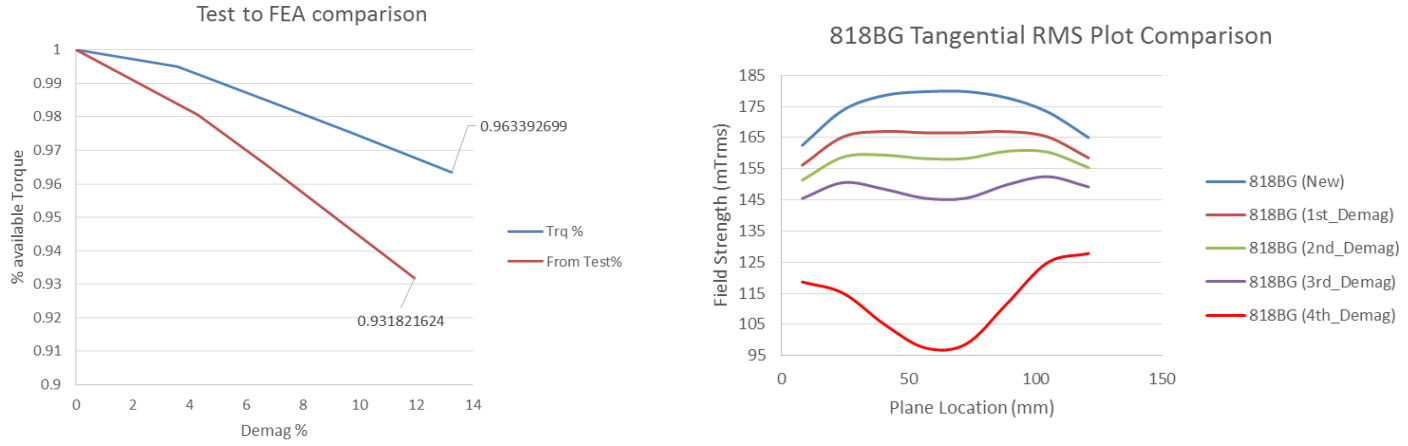

Figure 13: Predicted demagnetization compared to experimental results, left. Field measurement of sequential demagnetization tests along the motor axis, right.

Motor Testing

All rotors were tested at high speeds to ensure rotor strength. The testing results are shown in Table 4. All rotors demonstrated capability beyond the rated speed and were tested until failure.

Table **Error! No text of specified style in document.**.2 Rotor overspeed testing

Test unit	Type	Speed 1	CMM	Speed 2	CMM	Speed 3	CMM	Ramp Speed to Failure
1	Variant 1 HRE-free PM							*
2				*				
1	Variant 2 (SyRM w PMA)							*
2								*
1	Variant 3 (IM)							*
2						*		

* indicates test step at which rotor rub occurred

Table 4: Rotor overspeed testing

Figure 14: Rotors post-test. Each rotor was tested until failure

Variant 1 – HRE-free Permanent Magnet Motor Performance

The Variant 1 Motor was tested at voltages from 250V to 350V. The efficiency of the Variant 1 motor, shown in Figure 15, is high, consistent with other permanent magnet motors. Power is slightly below the predicted power of 148kW, but the requirements are still met for this motor.

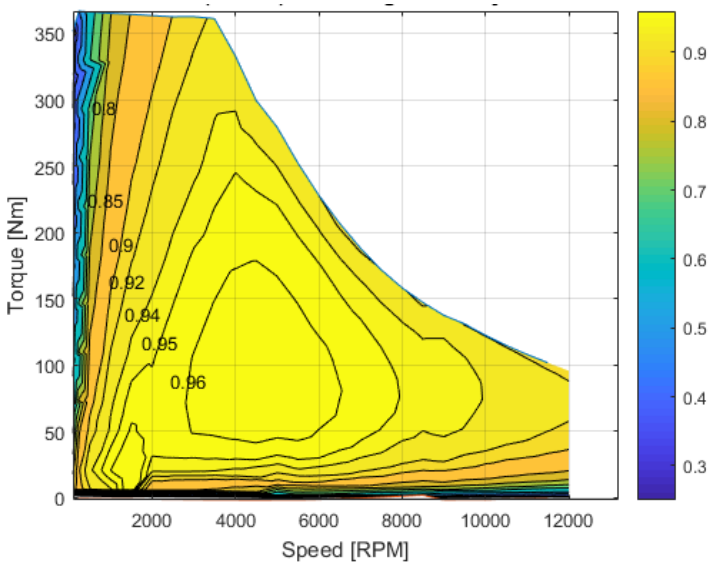

Figure 15: Performance of Variant 1 motor, tested at 350V

Demagnetization testing was completed with the motor exposed to significantly higher temperatures than those expected during normal operation, and under adverse currents. These results provide good confidence that this motor, with HRE-free magnets, would be able to operate in vehicle conditions.

Overall, the motor meets the specific power, power density, and cost targets as defined in the FOA, 2019 AOI 5_1384-1599.

Performance						
	Mass	**Volume**	**Power**	**Specific Power**	**Power Density**	**Cost**
Target				≥1.6 kW/kilogram	≥5.7 kW/Liter	$4.7/kW
Variant 1	35.2 kg	6.6 L	146 kW	4.1 kW/kg	22.1 kW/L	Meets

Table 5: Summary of Performance to requirements for Variant 1 Motor

Variant 2 - Synchronous Reluctance Motor with HRE-free PM Assist

The efficiency of the Variant 2 motor, shown in Figure 16, is high, with a maximum efficiency of 96%, and demonstrates overall higher efficiency than induction motors of similar sizes, and high-speed efficiency regions consistent with an intended usage as a secondary motor or e-axle operation.

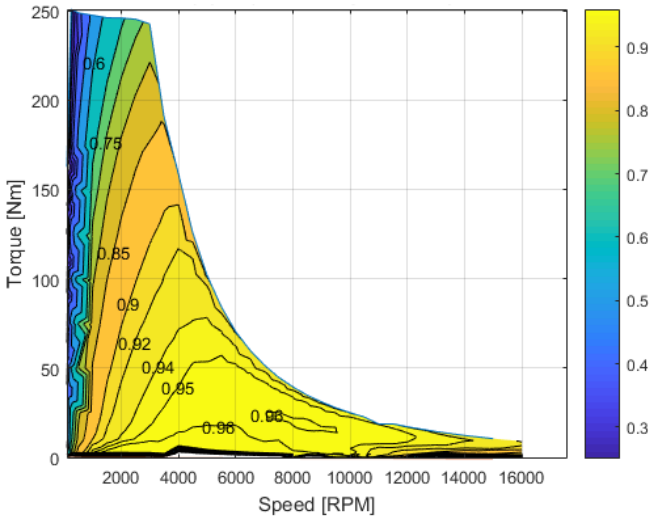

Figure 16: Performance of Variant 2 motor, tested at 350V

During demagnetization testing, the motor was ramped to temperatures significantly above those predicted by multiple wide-open throttles, resulting in no significant demagnetization to the motor under adverse conditions. The rotor topology therefore shows significant protection to the magnets, enabling the use of lower coercivity magnets and no heavy rare-earth materials.

High-speed fatigue testing was also completed for the Variant 2 motor. Although the scatter was relatively high for these rotors, this is perhaps due to the prototype stamping of these parts. The number of cycles to failure for these parts at the speed they were tested show promise for their potential application. Figure 17 shows the failures of the motors after high-speed cycling.

Figure 17: Variant 2 rotor after rotor endurance failure.

While the specific power and power density targets are met for this application by the rotor design, cost targets remained a challenge to meet, as shown in Table 6. The cost target is difficult to meet for this motor due to the lower peak power of the motor compared to the Variant 1 design.

Performance						
	Mass	**Volume**	**Power**	**Specific Power**	**Power Density**	**Cost**
Target				≥1.6 kW/kilogram	≥5.7 kW/Liter	$4.7/kW
Variant 2	24.1 kg	5.4 L	76 kW	3.15 kW/kg	14.1 kW/L	Does not meet

Table 6: Summary Performance to requirements for Variant 2 motor

Variant 3 – Hybrid Induction Motor with Insert Cu bars and Cast Al End-rings

The efficiency of the Variant 3 is as predicted at 92% and shown below in Figure 17. This higher efficiency is driven primarily by the copper bars improving the conduction losses of the rotor. In addition, the high efficiency region is notable in the high-speed regions, consistent with one of the possible applications of the motor.

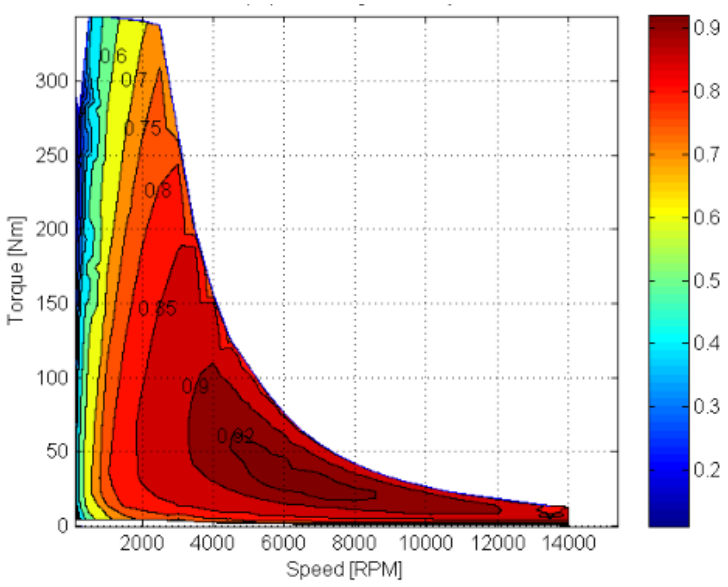

Figure 17: Performance of Variant 3 motor

The motor was run at repeated cycles at high speed until failure. Cracking occurred at the end-rings, likely initiating at the interface between the cast aluminum and the copper bars as shown in Figure 18.

Figure 17: Variant 3 rotor after rotor endurance failure

Like the Variant 2 motor, while the specific power and power density targets were met by this motor design, the cost remained a challenge, driven primarily by the cost of the copper bars and the lower power of the induction machine.

Performance						
	Mass	**Volume**	**Power**	**Specific Power**	**Power Density**	**Cost**
Target				≥1.6 kW/kilogram	≥5.7 kW/Liter	$4.7/kW
Variant 3	27.3 kg	5.4 L	84 kW	3.2 kW/kg	16.3 kW/L	Does not meet

Table 5: Summary Performance to requirements for Variant 3 motor

Oakridge National Lab (ORNL) testing

Background and Ongoing Efforts

ORNL continued working with steel samples and copper/aluminum bars that were provided by GM for materials analysis. GM previously provided various sample sizes and shapes for three steel products for metallography, mechanical testing, and electromagnetic testing. Earlier in the project, tensile tests were performed on a single sample of each of the three candidate materials. Five additional samples for each material (15 total) underwent tensile testing at room temperature. Fatigue testing of 20 samples per material (60 total) were completed. These tests were performed with load control at 50 Hz with a sinusoidal waveform and were discontinued after 10,000,000 cycles. Upon failure, each sample is inspected with SEM to show crack initiation location and any grain orientation at the crack initiation site. The resulting stress live curves are shown in Figure 18, showing that the fatigue life of material “C” is generally greater than that of material “B”, and the fatigue life of material “B” is generally greater than that of material “A” for all tested stress levels.

Upon failure, each sample was inspected with SEM to analyze crack initiation location and any grain orientation at the crack initiation site. Furthermore, microscopy and microhardness measurements were performed on the edge of the samples to inspect for cleaved grains, various deformation patterns, and to determine a distribution hardness and investigate residual stress as a result lamination stamping action. Compositional analysis of the bulk material of the sample, as well as the coating was also performed. Coating thickness and overall sample density were determined.

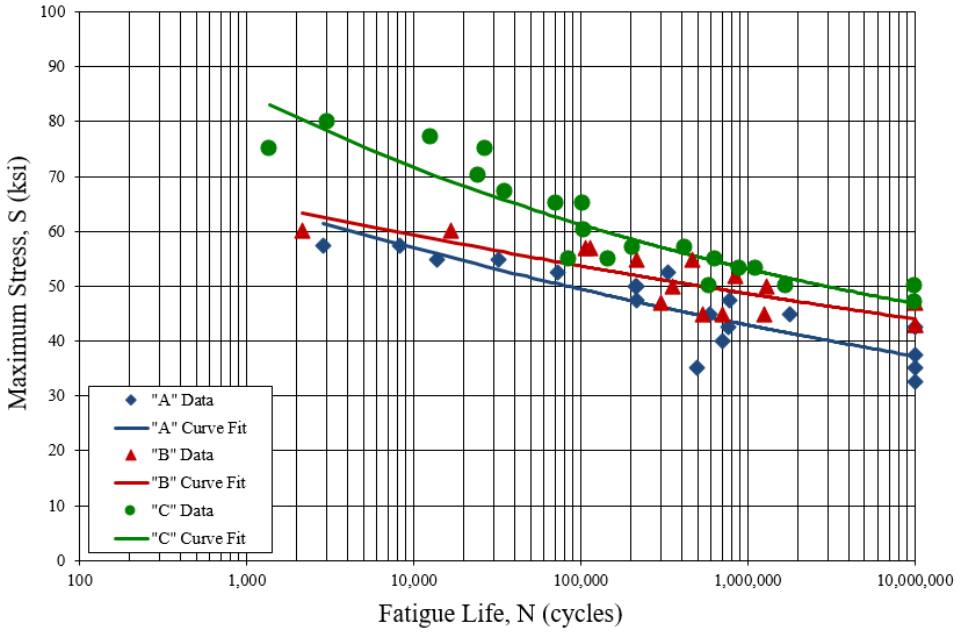

Figure 18: Stress life curves for materials "A", "B", and "C

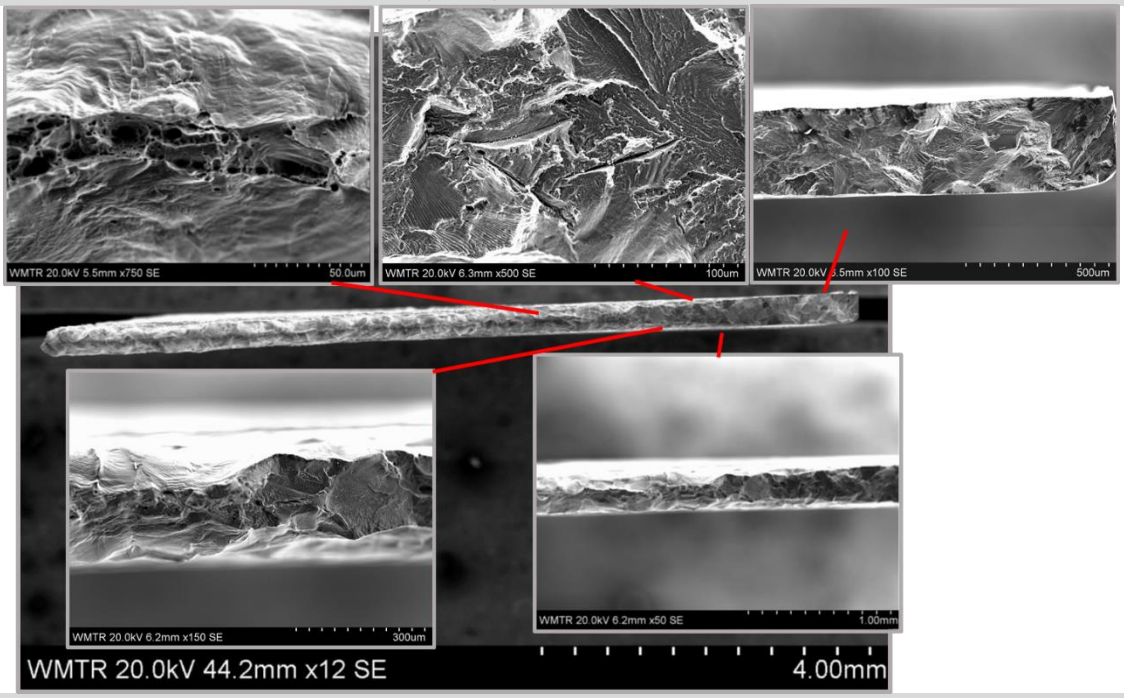

Figure 19: Example of fracture analysis with SEM for material A, sample #2.

3D Analysis of Single Bar Samples with X-Ray CT Scanning

GM provided ORNL with single bar samples (shown in Figure 19) that were prepared for porosity analysis. X-Ray CT scanning faces the similar issue as CT scanning with neutrons. In this case, the sample was small enough not to sufficiently attenuate the X-Ray beam during analysis. Scanning of one bar has been completed, and a reconstructed 3D rendering is shown in Figure 20. Both left and right images are 3D renderings at the same angle, with the left image having no object (Al and Cu) opacity and the right image with higher opacity to distinguish the orientation of the sample. The data was analyzed to determine pore size and distribution throughout the sample. A visual inspection shows that while large voids were present near the tab-like features of sample, there were very few and small voids at the Cu-Al interface, the critical area of interest.

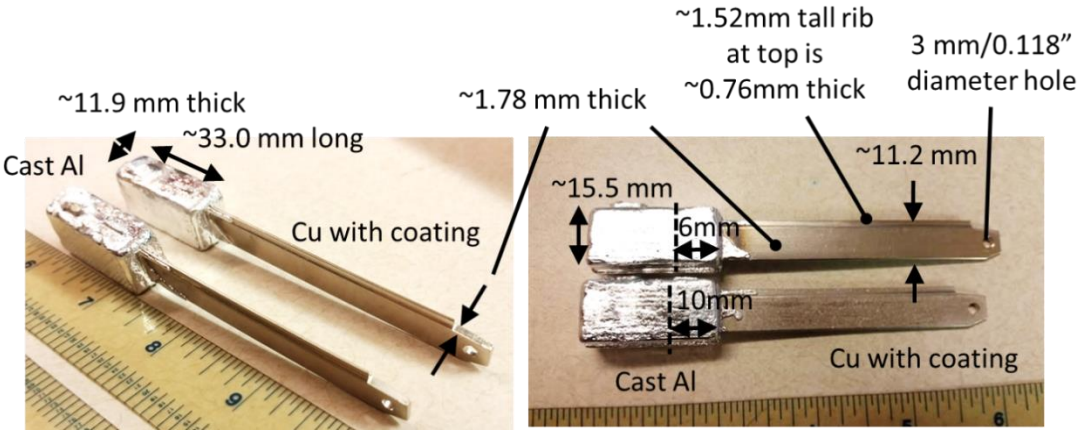

Figure 19: Rotor bar casting sample.

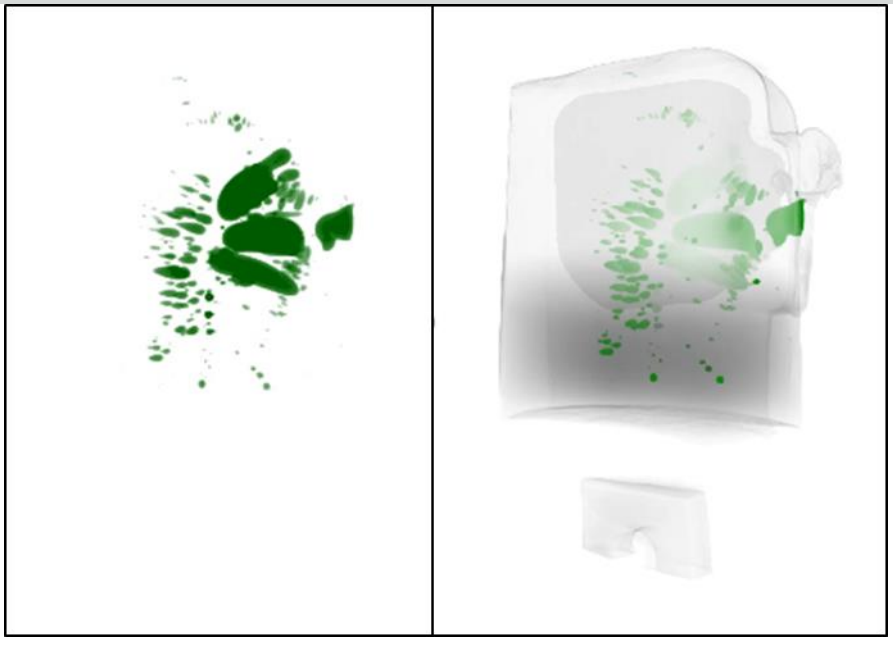

Figure 20: X-ray CT scanning results from rotor bar sample

Steel testing

A series of tensile tests were conducted with three candidate materials on the most readily available equipment shown in Figure 20. Processed stress-strain curves are shown in Figure 21, and the correlating mechanical properties from the tensile tests are shown in Table 6, Figure 22, and Figure 23. The material 46185-2 has a much higher ultimate tensile strength (UTS) of 604 MPa when compared to a UTS of 486 MPa and 427 for materials 54424-2 and 55006-2, respectively. It is important to note that this test setup is typically used with larger samples with higher force requirements, and therefore, raw data from the tests indicates considerable variation in the stress-strain as a result of the sensor, actuator, and feedback system being intended for larger loading. A smaller tensile test frame became available, and more extensive testing including multiple samples for repeatability was also conducted.

Figure 20: First Tensile Test Setup

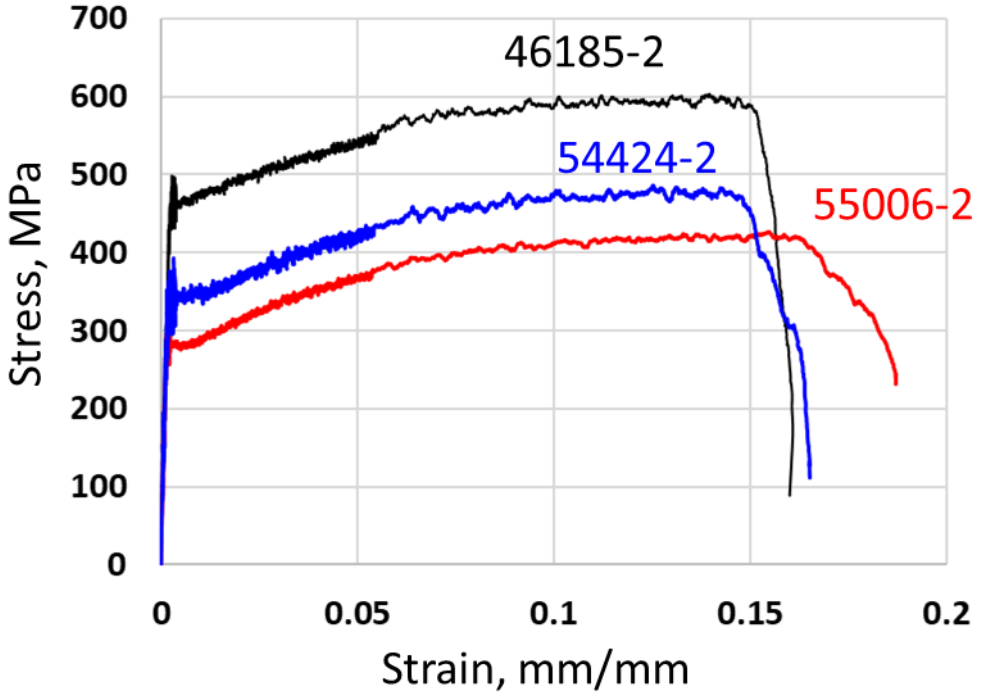

Figure 21: Comparison of stress-strain curves of three candidate materials

Parameter	46185-2	55006-2	54424-2	Notes
0.2% Yield, MPa	463	281	338	
UTS, MPa	604	427	486	
Total Elongation	0.161	0.187	0.165	
Uniform Plastic Strain	0.143	0.153	0.124	End of linear part to max uniform strain
E, GPa*	190	190	190	*The elastic modulus from first tests was not accurate due to large noise, it is 190GPa with about 10% variation

Table 6: Comparison of Properties from First Tensile Tests.

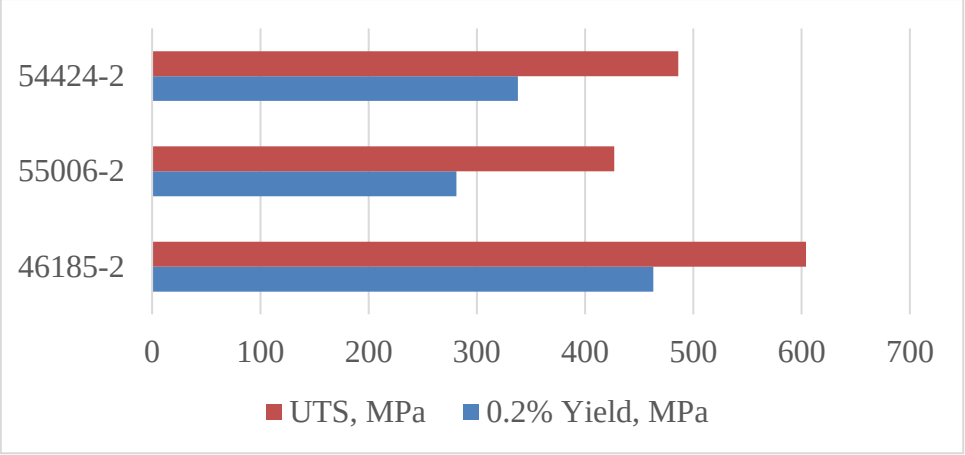

Figure 22: Comparison of ultimate tensile strength and 0.2% yield for three candidate materials.

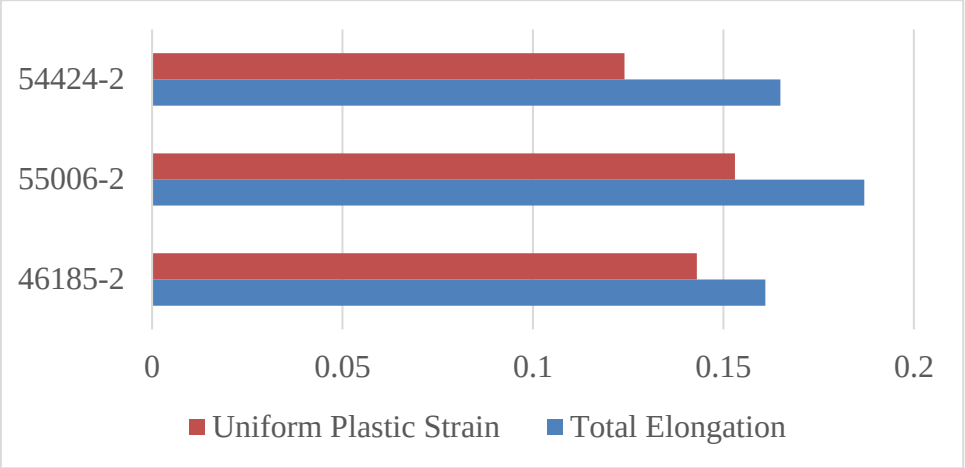

Figure 23: Comparison of uniform plastic strain and total elongation for three candidate materials.

Rotor bar tensile and fatigue testing

Based on guidance from GM, ONRL designed and fabricated a custom test fixture to grip rotor bar test specimens for tensile and fatigue testing. Tensile test data is shown in Figure 24 and it is shown that the average maximum loading is quite close between the two variants (3,610.6 N and 3,586.6 N for Batch #1 and #2, respectively), but the average displacement is considerably different, with an average of 19.69 mm and 14.23 mm for Batch #1 and #2, respectively. Inspection of the failed tensile specimens indicated that all Batch #1 specimens failed near the center of the copper bar, while all Batch #2 specimens failed in the copper bar near the cast interface.

Figure 24: Custom test fixture made for testing rotor bars

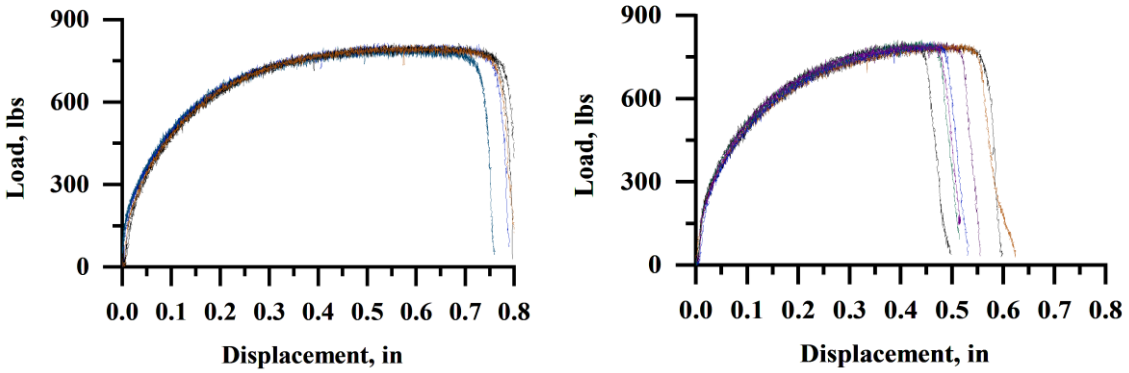

Figure 25: Rotor bar tensile test results, Batch #1 (left) and Batch #2 (right).

Edge Microscopy

Edge microscopy of the stamped edge was performed on the gauge section. Two samples for each material were inspected. Scanning electron microscopy (SEM) with secondary electron image (SEI) was used to obtain more detailed topographical information. Observations were made to identify rollover, shear, tear/fracture zones, and burr. Measurements for the first sample of material A ("A1"), are shown in Figure 26.

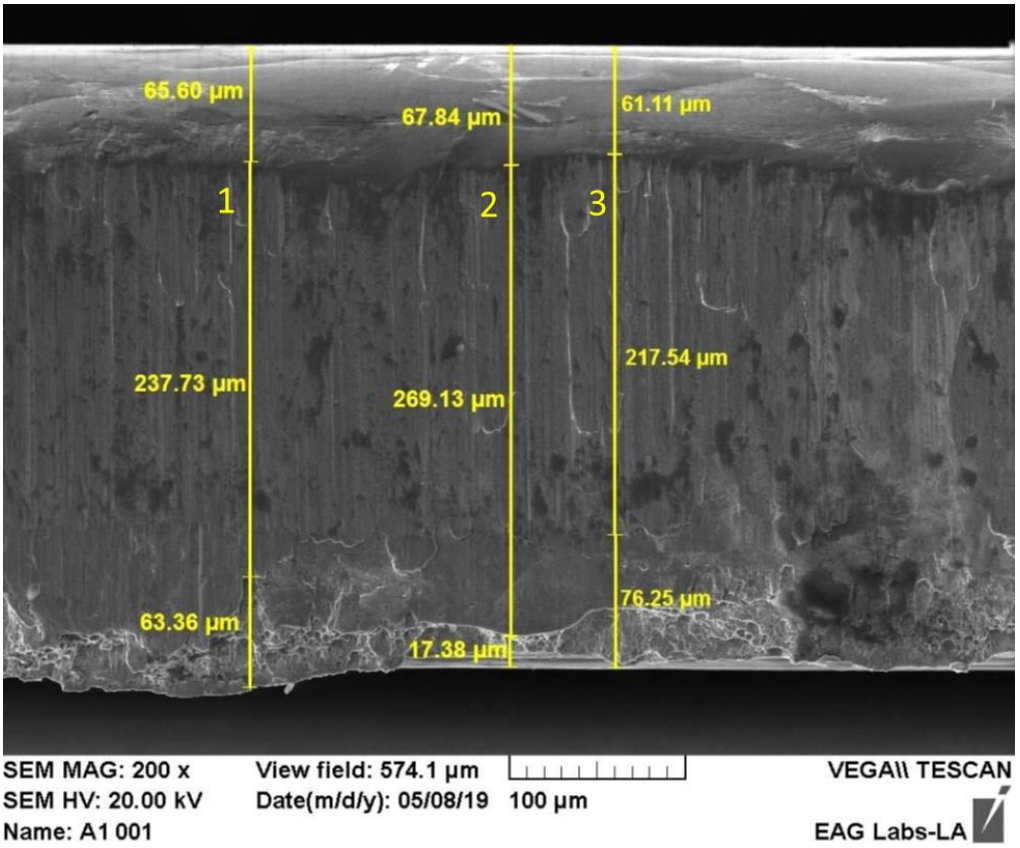

Figure 26: SEM SEI image showing Sample A1 measurement sets 1-3 at 200X magnification.

Magnetic steel testing

GM provided Epstein and single sheet tester (SST) lamination steel samples for electromagnetic testing. The Epstein test frame is shown in Figure 27. Testing was performed in accordance with ASTM A343, as masses and other measurements of the specimen were made prior to testing. The key purpose of these tests was to provide a comparison of magnetic properties between materials and to compare magnetic properties between the same materials that have and have not been subjected to stress-relief annealing (SRA).

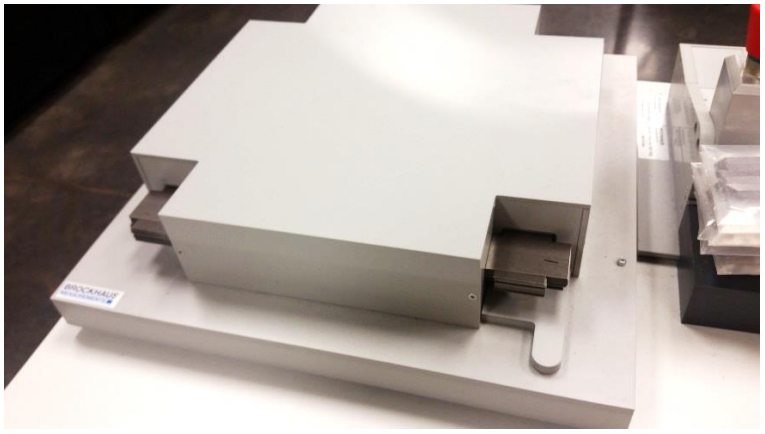

Figure 26: Epstein test frame

The SST (single strip tester) frame, shown in Figure 26, offers much faster setup time and a wider testing range due to the smaller sample size and much less volume required to magnetize. The method was used for both stress-relief annealed (SRA) and not-SRA (NSRA) variants. A comparison of test results with strip quantities provides insight into the impact of residual stresses from punching action, as it is typical for residual stresses to negatively impact the magnetic characteristics of lamination steel. Furthermore, these tests provide insight into the effectiveness of the SRA process to restore magnetic properties by mitigating residual stresses.

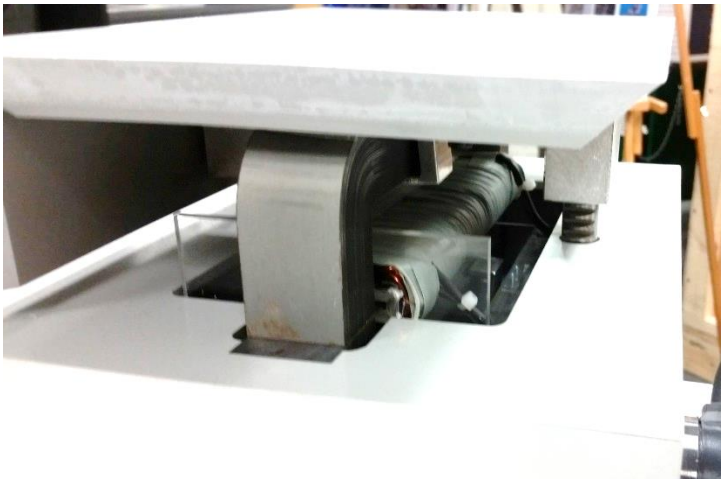

Figure 26: SST Frame

CONCLUSIONS

GM completed the design, prototype manufacturing, and testing of the three motor variants, which all resulted in close results to the predicted power and efficiency values. Motor variants 1 and 2 show good resistance to demagnetization using HRE-free magnets, a key objective of the project. Variant 1 showed good success in meeting the cost and performance targets. In addition, mechanical sacrifices necessary to improve power in the Variant 2 and efficiency in the Variant 3 motors were found to be acceptable from the perspective of rotor efficiency, but cost remained a challenge for these motors.

Networks or Collaborations Fostered

Collaboration with Oakridge National Laboratory for materials testing

Patent Application Summary

One invention was conceived during the project. Patent application status is summarized below:

Invention No.	Country	Patent Application	Date	Patent	Issued
	US	15/895400	2/13/2018	10886802	1/5/2021
S-162,977	Germany	102019102993.7	2/6/2019		
	China	201910108463.2	2/3/2019		